3.4 Fluid Dynamics

Group Leader: Jonathan Freund

Faculty: S. Balachandar, Daniel Bodony, Jonathan Freund, Robert D. Moser, and S. Pratap Vanka

Research Scientists: Andreas Haselbacher, Fady Najjar and Bono Wasistho

Postdoctoral Associate: Babak Shotorban

Graduate Students: Prosenjit Bagchi, Henry Chang, Zhiqun Deng, Heath Dewey, David Lin, Victor Topalian, Prem Venugopal, Lulama Wakaba, Paulo Zandonade, Lanying Zeng, Lin Zhang, and Hong Zhao

Overview

The Fluid Dynamics Group works on system-scale solid rocket motor multiphase compressible core flow code development, as well as subscale model development relevant to the turbulent dynamics of the combustion interface. This includes research projects that intersect with the integrated code in injection, dispersion and combustion of aluminum droplets in the core flow; formation, dispersion and slag accumulation of aluminum oxide particles; and flow within cracks and other defects within the propellant.

Rocflo and *Rocflu* Development

Enhanced Multiphase Flow Computational Framework for Mixed Unstructured Meshes (Najjar, Haselbacher, and Balachandar)

The operating environment inside the chamber of solid-propellant rocket motors (SRM) presents a particularly interesting example of multiphase flow. Propellants in modern SRMs are enriched with aluminum particles to increase the specific impulse and damp combustion instabilities. As the propellant burns, aluminum particles melt, agglomerate, and collect as droplets at the propellant-combustion interface. Droplets of aluminum are then entrained into the high shear flow when flow-induced lift forces exceed surface tension forces. The initial droplet size typically varies from tens of microns to a few hundred microns. At the high temperatures typically encountered in the chamber, the aluminum droplets vaporize and react with various oxidizing agents. The primary products of combustion are micron-sized aluminum oxide particles. Understanding the behavior of aluminum droplets and aluminum-oxide particles is quite important in the SRM design and analysis. For example, the impact of oxide particles on the nozzle walls can lead to scouring. Also, aluminum droplets can accumulate in submerged nozzles as slag. At motor

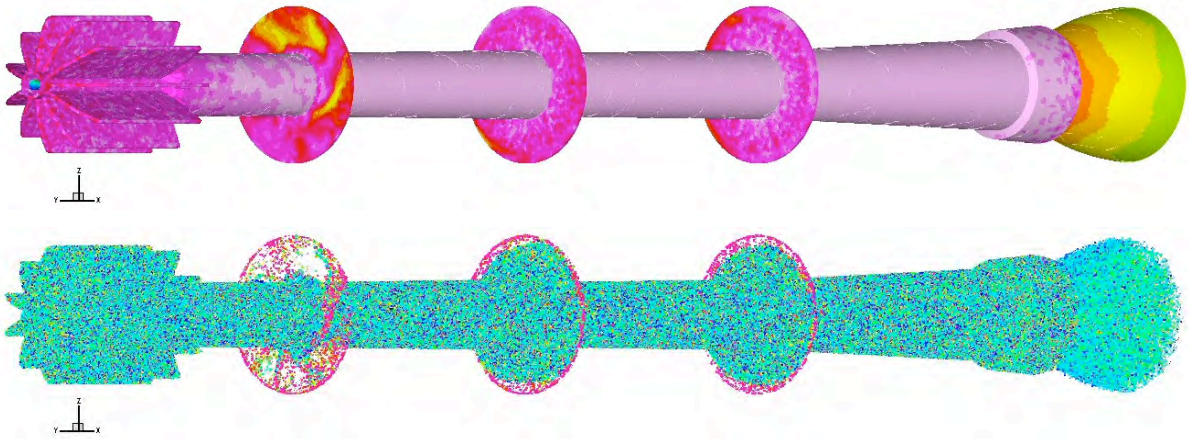

Fig. 3.4.1: Results for RSRM motor configuration at t=0 using unstructured fluid solver, *Rocflu*:(top) static temperature of mixture (K), (bottom) droplet positions colored by droplet diameter.

burn-out, the rapid pressure reduction can lead to the ejection of the slag accumulated in the nozzle bucket, forming space debris.

Being able to track these Lagrangian droplets on unstructured grids with complex geometries is a challenging task. A ray-tracing algorithm is developed addressing these deficiencies while maintaining efficiency. The approach considers the intersections of the particle trajectory with the faces of the underlying grid. Together with a face-based data structure, the intersection point on a face directly indicates the cell into which a particle is moving. By focusing on intersections with faces, the algorithm deals with boundaries in a natural way. Efficient memory management using dynamic memory reallocation has been developed for *Rocpart*. Further, a scalable MPI-based parallel algorithm was developed permitting the droplets to move through indefinite number of regions residing on many processors with relative ease. The framework has been enhanced to handle droplet impingement on nozzle walls, while capabilities to track droplets being trapped in the bucket of a submerged nozzle are currently being pursued. Verification problems have been performed showing that the algorithm is third-order accurate in time and first (second)-order accurate for piece constant (linear) interpolation functions.

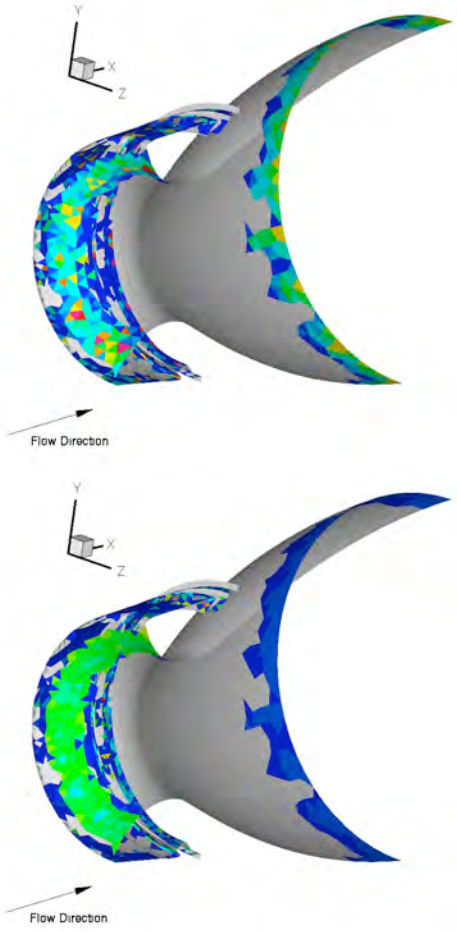

Fig. 3.4.2: Droplet impact statistics on CD nozzle: (top) Number of hits (bottom) diameter.

These multiphysics capabilities have been integrated with the unstructured flow solver, *Rocflu*, and simulations for several motor configurations, including the 70-lb AFL BATES and 11-star RSRM motors, have been performed. Figure 3.4.1 shows the mixture temperature field, and the droplet location (colored by diameter size) for the RSRM configuration at t=0. It is seen that the static temperature is quite uniform in the chamber dropping rapidly in the CD nozzle. In Figure 3.4.1 (bottom), approximately 4 million droplets are being tracked with the parallel MP framework. Large-sized droplets are seen to be trapped in the first slot (since the propellant is inhibited); while the second and third slots are fully populated by burning droplets. Moreover, a significant number of droplets are seen in the nozzle bucket due to the presence of burning propellant. Figure 3.4.2 (a) and (b) show the cumulative number of hits for the droplets impinging on the nozzle walls and their corresponding diameters.

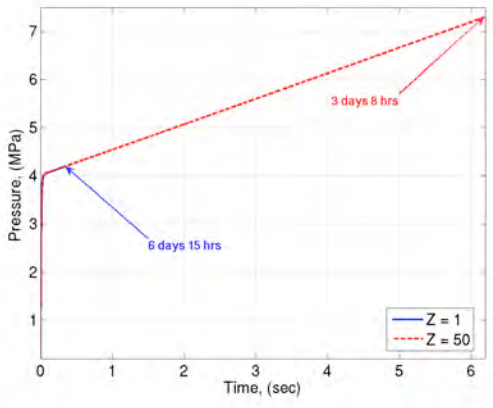

Fig. 3.4.3: Time-variation of head-end pressure for cylindrical rocket motor with no slow time acceleration (Z=1) and slow-time acceleration factor of Z=50. CPU time required to attain burn time is also shown.

Slow-Time Acceleration Method to Enable SRM Burn-Out (Moser, Haselbacher, Najjar, and Massa)

Detailed first-principle computations of the flow in solid-propellant rocket motors (SRM) are

challenging because of the wide range of length and time scales. In our computations, the time scale of primary interest is that of the evolution of turbulence. This time scale is much faster than the burn-out time scale, which makes the simulation of SRM burn-out including turbulence very time-consuming. A detailed analysis of all the physical and numerical time scales suggests that an approach based on multi-scale asymptotics can be used to accelerate burn-out computations. Hence we have developed a new approach which allows acceleration of slow-time scales while leaving the evolution of fast time scales unchanged. Application of this approach to a simple SRM with center-perforated grain exhibits measured accelerations of up to a factor of 36. Our new approach is applicable not only to SRM computations, but to any physical system with widely separated time scales and for which the dynamics of the fast time scales are of primary interest. In the slow-time acceleration method, we consider a system that exhibits multiple time-scale behavior, with at least one very large time scale, and for which the dynamics of the fast time scale is of primary interest. Thus we would like to be able to accelerate the slow-scale evolution while preserving the dynamics of the fast time scale.

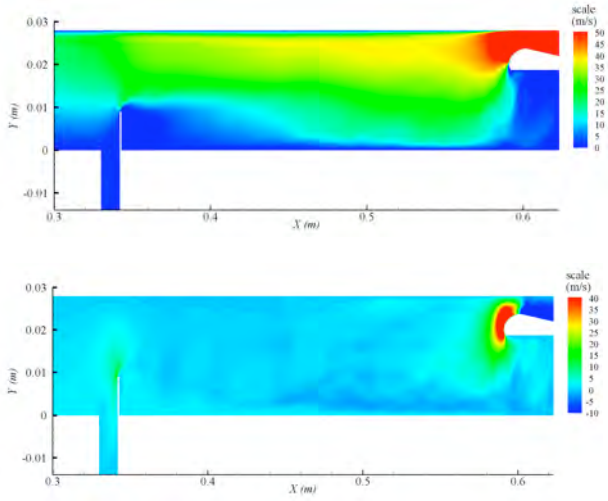

Figure FMN5: Distribution in y=0-plane for mean components of (top) streamwise and (bottom) cross-stream velocities.

Large-Eddy Simulations of Wall and Shear-Layer Instabilities in a Cold Flow Motor Setup (Najjar, Plourde*, Wasistho, and Balachandar) *Collaborator from CRNS-ENSMA, Universite de Poitiers, France.

Large-eddy simulations of a solid rocket motor scale model are being performed in order to characterize the effects of turbulence on the sources of instabilities. The scale model is based on a cold gas experimental set-up reproducing the main geometric features of a segmented motor. The presence of inhibitors triggers a vortex shedding phenomenon in its wake while the main flow close to the injection wall supports a wall vortex shedding dynamics arising from the hydrodynamic instability. Computations are being performed with *Rocfluid*-MP while the LES turbulence module, *Rocturb*, has been invoked. A mesh resolution of over 3million grid cells is considered; while random turbulence fluctuations with an amplitude of 20% is injected over the mean value to maintain the three-dimensionality characteristics of the flow.

The mean field was computed by performing averaging from t=16 to 30ms with a sample size of 0.01ms; hence the field has been averaged over 2000 time steps. Figure FMN??(a) & (b) show the distributions of the mean x- and y-velocities and pressure in the mid-plane (y=0), respectively. It is clearly seen that the development of the shear-layer from the inhibitor reattaching further downstream (around x=0.47m); while for the vertical velocity, a high component is observed on the nozzle wall. Figure FMN?? (a) & (b) presents the rms field in the streamwise and cross-stream direction, respec-

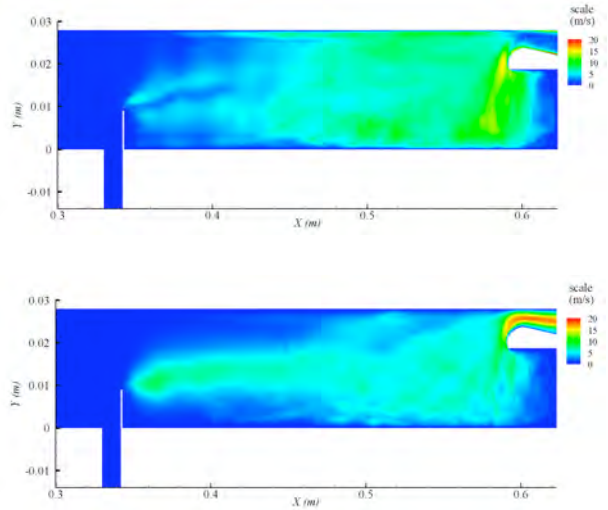

Figure FMN6: Distribution of the RMS field in y=0-plane

tively. It is seen that the development of the shear-layer acts strongly in generating fluctuations although the streamwise rms field has low values downstream of the inhibitor. In fact, the field is strongly amplified in the rear-part of the chamber where maximum levels are reached. However, for the cross-stream rms field, a more structured distribution is observed: back to the obstacle position, levels develop in the wake of the obstacle and spread mainly towards the injecting walls and at $X = 0.4$ approximately, vertical fluctuating activity are observed to be inclined against the injecting wall boundary conditions. Finally, Figure FMN7 shows 3D perspectives of the iso-vorticity contours. We can be clearly observed the vortex shedding development as well as the rapid transition from a laminar flow to turbulence.

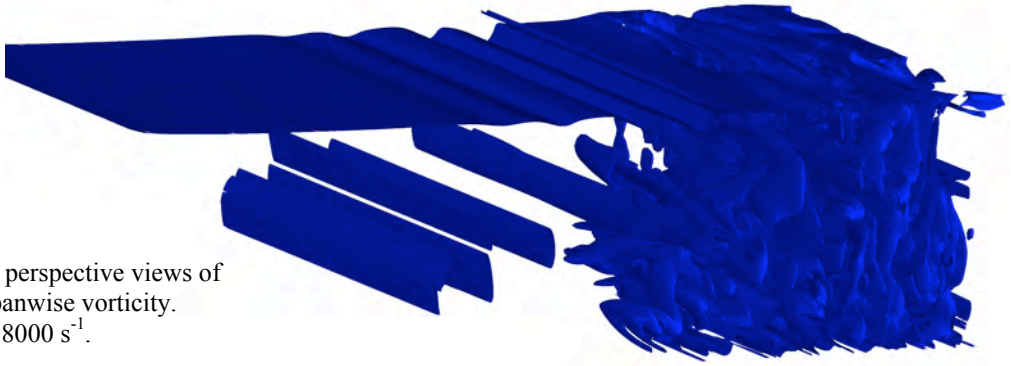

FigureFMN7: 3D perspective views of iso-contours of spanwise vorticity. Contour Level of 8000 s^{-1}.

Need title and authors

We have investigated two approaches to improve the simulation of turbulence and other multiscale flow-physics phenomena within Rocflu. The first has been to implement locally one-dimensional finite difference stencils in locally structured regions of the otherwise unstructured mesh. This permits the use of high-order and, more importantly, non-dissipative numerical methods in regions of the flow. This approach works, but it is still somewhat limited in the range of geometries and flows that can be easily simulated. In essences, the mesh generation difficulty we seek to avoid by using the unstructured-mesh solver once again becomes a challenge. The second approach, therefore, has been to implement a recently proposed non-dissipative unstructured-mesh algorithm. It works on arbitrary unstructured meshes without artificially dissipating kinetic energy and thereby damping the turbulence. It is up and running in a stand-alone code and work proceeds implementing it into Rocflu. Figure <turb.jpg> shows a result from an unstructured flow solver on isotropic turbulence. A standard unstructured flow solver would have damped the turbulence excessively (there would be no contours to see) by this point, whereas this method has simulated it accurately for 30 large-eddy turn-over times with negligible numerical dissipation.

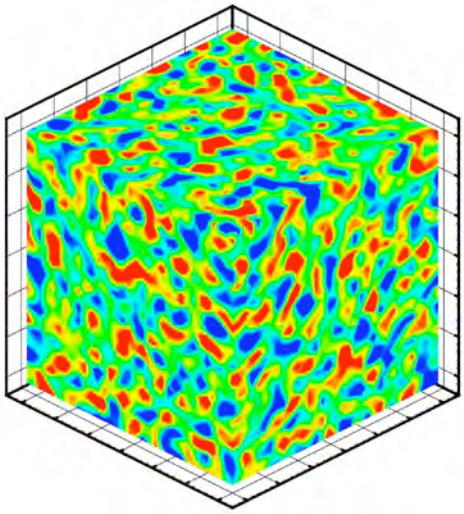

Figure <turb.jpg>. Vorticity in periodic box of turbulence simulated on unstructured mesh with non-dissipative numerical scheme.

We have also continued our efforts developing staggered-mesh high-resolution non-dissipative numerical methods for the simulation of turbulence in rocket motors as well as other applications. We finished an assessment of boundary conditions and recently implemented a shock-capturing scheme that is designed to accurately represent shocks with minimal impact on turbulence. (Many standard shock capturing schemes see any small-scale fluids structure as a shock and unnecessarily add excessive dissipation.) In a rocket, shocks are important in the nozzle

and plume. Our formulation is also directly compatible with high-order chimera mesh schemes, which are under investigation. We have demonstrated our implementation in a two-dimensional jet simulation, results of which showing the shock-cell potential core structure are visualized in figure <jet.jpg>.

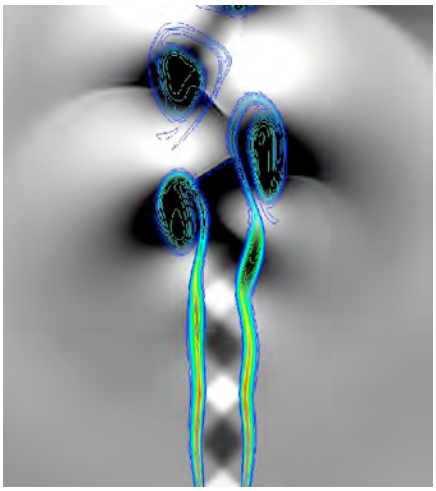

Figure <jet.jpg>. Two-dimensional under expanded jet demonstrating shock capturing: vorticity and pressure.

We have begun to investigate means of gaging the sensitivity of simulation results to input parameters. This is a key step to undertaking truly predictive simulations. In a complex system such a solid rocket motor, the relative sensitivity of the results to different input parameters (geometry, burn temperature boundaries, etc.) allows us to focus on the most important parameters to assess the overall uncertainty of the result. Doing this directly in the most straightforward way would require multiple simulations, one for each parameter to be varied. However, if formulated correctly the adjoint of the governing equations can provide the needed sensitivity for all input parameters with a single solution. We have formulated the adjoint of the compressible flow equations, for now in a stand alone code, and developed an appropriate high-resolution algorithm to solve it. We have studied the propagation of a sensitivity field, here the sensitivity of the noise radiated by a turbulent mixing layer, to local changes in the flow. This field can then be used at boundaries and elsewhere to assess to which parameters the solution is most sensitive. This information can thus indicate which parameter sensitivity to study in greater detail in order to assess the overall uncertainty in the method.

The simulation of finite deformation fluid-structure interactions is challenging because it requires the matching of the solutions of the governing equations for the fluid and solid at changing and a priori unknown positions. We have developed a new strategy for doing this. The philosophy behind it is simple: write the the conservation laws in a single unified form and use a separate numerical formulation only for the terms that are different in the solid and fluid regions. Since the basic conservation laws (mass, momentum, and energy) apply universally, the corresponding governing equations can be formulated in nearly the same way in solids and fluids. With essentially the same governing equation in the two portions of the solver, the coupling is significantly simplified. We solve the momentum equation on a fixed Cartesian mesh in both regions. Thus, the solver can to be fast, accurate, and non-dissipative. The constitutive model for the elastic solid depends upon its reference conditions, which can most easily be tracked with a moving Lagrangian mesh. We use finite elements to discretize the constitutive relation. This overlaid mesh approach is shown schematically in figure <mesh.jpg>. A projection method, which exactly preserves conservation of momentum, is used to transfer the divergence of the solid stress to the Carte-

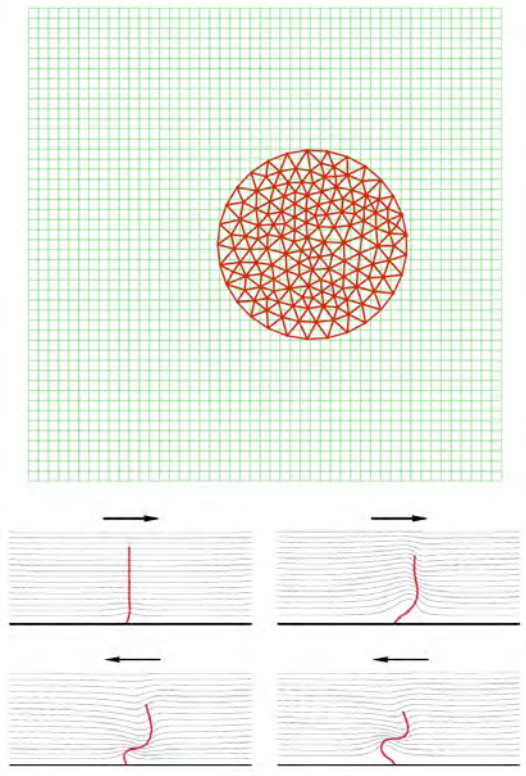

Figure <mesh.jpg> & <leaflet.jpg>. (top) Overlaid mesh schematic and (bottom) demonstration of flexible leaflet in oscillating flow.

sian mesh for time integrating the governing equations. Figure <leaflet.jpg> shows an elastic leaflet in a two-dimensional oscillating flow that was simulated using this method. For demonstration purposes this model system is constructed so as to deform even more than an inhibitor in a solid rocket motor.

A novel LES model consistent with equilibrium Eulerian formulation for simul ation of particle-laden turbulent flows (applications in the transport of smoke particles in solid-propellant rockets) (Shotorban)

To develop the new LES model, a filtered equilibrium Eulerian velocity is defined and calculated in terms of the filtered velocity and acceleration of the fluid phase and then it is used to solve the transport equation of the filtered particle concentration. The closure problem resulted from filtering the nonlinear convection term of particle concentration in the concentration transport equation and in the form of subgrid-scale particle flux, is modeled using the Smagorinsky kind of model. The assessment of the model is carried out in forced isotropic turbulence. The LES model results are well compared against results obtained by DNS.

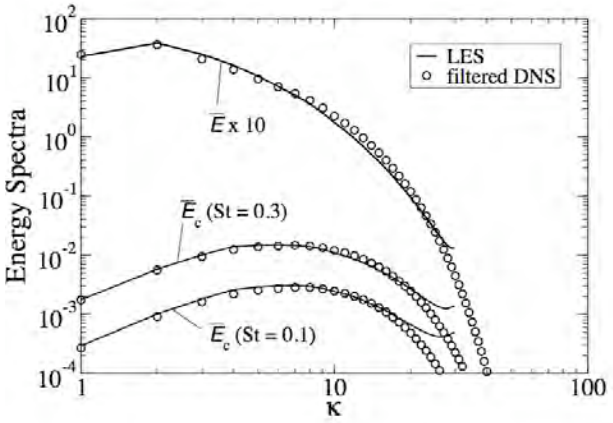

Figure 1 Energy spectra of velocity field and particle concentration field in forced isotropic turbulence for two different Stokes numbers.

A novel equilibrium Eulerian model for DNS of particle-laden turbulent flows in two-way coupling (applications in the transport of smoke particles in solid-propellant rockets)- (Shotorban)

A model based on the Equilibrium Eulerian formulation is developed to account for the modification of the fluid-phase turbulence under the influence of particles (two-way coupling). For the assessment purposes, a decaying particle-laden isotropic turbulent flow is studied. The results obtained through the proposed new model are compared against those obtained by the trajectory approach in which particle equations are solved in the Lagrangian framework. It is shown that there is a good agreement between these two approaches for various small Stokes numbers and mean particle concentrations. Figure 2 shows the time evolution of dissipation rate of the turbulent kinetic energy in the decaying isotropic turbulence for various particle Stokes numbers and the mean particle concentration.

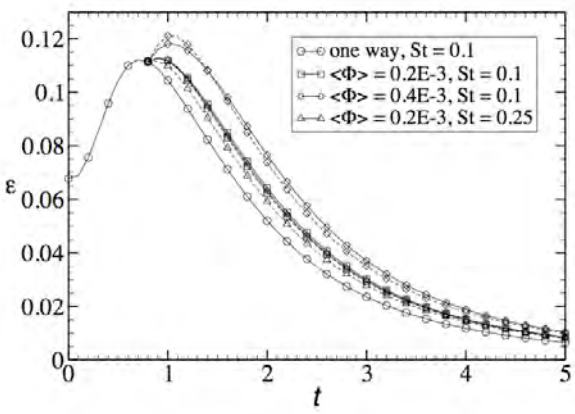

Figure 0 - Equilibrium Eulerian (solidline) and Lagrangian (dashedline